Polyelectrolyte complex membranes made of chitosan—PSSAMA for pervaporation separation of industrially important azeotropic mixtures

Divya Achari[a], Padmeshwary Rachipudi[a], Satishkumar Naik[a], Ramesh Karuppannan[b], Mahadevappa Kariduraganavar[a,*]

[a] Department of Chemistry, Karnatak University, Dharwad 580 003, India
[b] Department of Physics, Indian Institute of Science, Bangalore 560 012, India

A B S T R A C T

Chitosan-based polyelectrolyte complex membranes (PECMs) were developed by incorporating polystyrene sulfonic acid-co-maleic acid (PSSAMA) in the chitosan membrane matrix as a pervaporation membrane by employing a solution technique. Fourier transform infrared (FTIR) spectroscopy, wide-angle X-ray diffraction (WAXD), thermogravimetry analysis (TGA), differential scanning calorimetry (DSC), and scanning electron microscopy (SEM) were used to characterize the membranes. PECMs were tested for their potentiality to separate various azeotropic mixtures; water/ter-butanol, water/isopropanol, water/n-propanol and water/1, 4 dioxane at their azeotropic point. The PECMs containing 9 mass% of PSSAMA manifest highest separation selectivity of 5352 with a flux of 4.145×10^{-2} kg /m^2 h for the azeotropic mixture of water/ter-butanol at 30 °C. To confirm their stability at the higher temperature, the PECMs were assessed for pervaporation (PV) separation at 40, 50 and 60 °C. For all PECMs total flux and flux of water appeared to be coinciding each other, signifying that PECMs could be used successfully to break the azeotropic point of various azeotropic mixtures. The Arrhenius activation parameters were determined by diffusion and permeation values. The activation energy values procured for water permeation (E_{pw}) were considerably lower than ter-butanol permeation (E_{pTBOH}). The heat of sorption (ΔHs) values obtained for PECMs were negative, showing that Langmuir's mode of sorption is dominant.

© 2019 The Korean Society of Industrial and Engineering Chemistry. Published by Elsevier B.V. All rights reserved.

Introduction

During the last half-century, different types of separation processes have been developed and new processes are continually emerging from academic, industrial, and government laboratories. One of the most well-known membrane separation techniques that act as the core and key point of current membrane research is pervaporation (PV) [1–3]. PV is a membrane separation technology that is advantageous over the traditional distillation processes due to its energy-saving characteristic and the capability to proficiently separate the azeotropic mixtures with close boiling liquid mixtures, dehydrate organic solvents and concentrate aqueous solutions [4,5].

Today, the main application of PV in the membrane separation technology is the dehydration of aqueous-organic mixtures. Among the many aqueous-organic mixtures, the dehydration of alcohols (ter-butanol, n-propanol, isopropanol) and 1,4 dioxane have gained greater attention because of the increase cost and their importance in different industries. Alcohols (ter-butanol, n-propanol, isopropanol) and 1,4 dioxane are most important solvents used on a large scale in the chemical industries [6,7]. PV dehydration performance predominately depends on the manufacture of appropriate membranes with high permeability, good selectivity and adequate mechanical strength [8]. One of the superior candidates for dehydration of organics is polymeric materials with minimal cost, and significantly improved processability [9,10]. Hydrophilic polymers such as poly (vinyl alcohol) (PVA), poly (acryli cacid) (PAA), hydroxyl ethyl cellulose (HEC), sodium alginate (SA) and chitosan (CHS) [11–15] showed strong affinity towards water. A much-favored membrane material among them is chitosan due to its good film-forming properties,

Nomenclature

M. W.	Molecular weight
A	Effective membrane area (m^2)
DS	Degree of swelling (%)
D_o	Pre-exponential factor for diffusion
E_D	Activation energy for diffusion (kJ/mol)
E_{Dw}	Activation energy for diffusion of water (kJ/mol)
E_p	Activation energy for permeation (kJ/mol)
E_{pw}	Activation energy for permeation of water (kJ/mol)
E_{DIPA}	Activation energy for diffusion of IPA (kJ/mol)
E_{pTBOH}	Activation energy for permeation of ter-butanol
E_x	Activation energy for permeation or diffusion (kJ/mol)
ΔH_s	Heat of sorption (kJ/mol)
IPA	Isopropanol
J	Total flux (kg/m^2 h)
J_o	Pre-exponential factor for permeation
PSI	Pervaporation separation index
P and F	Mass percent of permeate and feed
R	Gas constant
t	Permeation time (h)
T	Temperature (K)
W	Mass of permeate (kg)
Ws and W_d	Mass of the swollen and dry membranes

Greek letters

δ	Membrane thickness (40 μm)
$\propto_{sep}$	Separation factor

sufficient mechanical strength, chemical resistance and high selectivity for water [16].

In order to prepare efficient pervaporation membranes, researchers focus on discovering new membrane materials with excellent properties. PECs, a multi-component polymeric material formed by the ionic complexation between oppositely charged polyelectrolytes, have been shown to be flexible membrane materials in pervaporation separation process. In the PV dehydration process, polyelectrolyte complex membranes (PECMs) are favorable candidates because of their ionic crosslinking structure, insolubility in common organic solvents, tunable surface energy and high hydrophilicity [17,18].

Literature indicated that various type of PEC membranes such as blend PECMs (BPECMs), two-ply PECMs (TPECMs), multilayered PECMs and homogeneous PECMs (HPECMs) were mostly employed in PV [17]. CHS-PAAc polyelectrolyte complex membrane for separation of 95% aqueous ethanol and obtained a permeation flux of 33 g/m^2 h with a separation factor of 2216 at 30 °C in the PV process studied by Shieh and Huang [19]. The separation of aqueous solution of alcohols through sodium alginate/chitosan PECMs reported by Lee et al. [20]. Kim et al. [21] mixed two anionic polysaccharides of sodium alginate and carrageenan (CG) in solution and stimulated the ionic interactions between sodium alginate and CG by adding Ca^{2+} as chelating ions. GKSS research institute, prepared TPECMs based on sodium cellulose sulfate (SCMC) and Poly (diallyl dimethyl ammonium chloride) (PDDA) [22] and other cationic polyelectrolytes such as poly (ethyl-eneimine hydrochloride) [23]. Recently, Li et al. [24] prepared SA–gelatin/ polysulfone (PSf) composite hollow fiber membrane and utilized it in dehydration of propylene. Meier-Haack [25,26] prepared multilayered PECMs on polyamide-6 and used them for the dehydration of alcohols and the separation factor for

water-2-propanol mixture was found to be 2500. According to Meier-Haack the higher the charge density of component polyelectrolyte, the higher is the selectivity in PV dehydration. Zhang et al. [27] prepared the hollow fiber PV membrane module successfully, and proposed a novel one-step potent assembly method for preparing PEC membranes based CHS [28]. Zhao et al. [29–32] prepared four processable PECs solutions by utilizing PAA, sodium carboxymethyl cellulose as an anionic polyelectrolyte and poly (2-methacryloyloxy ethyl trimethylammonium chloride) (PDMC), CHS as a cationic polyelectrolyte. Rachipudi et al. [33] prepared CHS based PECMs by immersing CHS membrane into phosphotungstic acid (PTA) solution. The permeation flux of CHS membrane was increased from 41.3 to 117 g/m^2 h and its separation factor was increased from 4490 to 7490 at 30 °C for dehydrating 10 wt% of water. More recently, Choudhari et al. [34], developed a PECMs with chitosan and PMAA for dehydration of 1, 4 dioxane and exhibited selectivity of 840 with flux of 12.07×10^{-2} kg/m^2 h at 30 °C for 15 wt% of water. Wang et al. [18] explained that PECMs containing $-SO_3^-$ groups showed a better PV performance than those containing carboxylate groups. Complexed $-SO_3^-$ groups improved the PV performance of PECMs for the dehydration of azeotropic mixtures.

Therefore, current investigation focuses on the preparation of PECMs containing sulfonate groups for PV separation of industri-ally important azeotropic liquid mixtures. We have made an attempt to develop PECMs by ex-situ crosslinking of CHS with Poly (4-styrene sulfonic acid-co-maleic acid (PSSAMA) with different weight ratio. PSSAMA acts as both a crosslinking agent and a donor of the hydrophilic group ($-SO_3H$). And also PSSAMA contains both strong acid ($-SO_3^-$) and weak acid ($-COOH$) groups and CHS containing amine (NH_3^+) and hydroxyl (OH^-) groups which were crosslinked via both esterification reaction and complex formation. The introduction of PSSAMA into the CHS polymer matrix can control the membrane charge density and also prevent excessive swelling [35,36].

The physicochemical properties of the resulting PECMs were studied with various techniques such as FTIR, WAXD, TGA, DSC, SEM, and Contact angle measurements and evaluated for PV separation of water/ter-butanol, water/n-propanol, water/ isopropanol, water/1,4 dioxane mixtures. The performance of the membrane is discussed by comparing and correlating the values of separation factor and the permeation flux. From the temperature dependence of permeation flux and diffusion coefficients, the Arrhenius activation parameters were estimated.

Experimental section

Materials

Poly (4-styrene sulfonic acid-co-maleic acid (Sodium salt) (M. W. = 20,000) and Chitosan (M.W. 2,00,000; N-deacetylation degree 75–85%) have been procured from Sigma-Aldrich, USA. Isopropa-nol, 1,4-dioxane, n-propanol, tertiary butanol and acetic acid have been purchased from S. D. Fine Chemicals Ltd., Mumbai, India. Only analytical grade chemicals were purchased and used as received. Throughout the study double distilled water has been used.

Membrane preparation

To obtain a transparent and homogenous chitosan (CHS) solution, 3 g of CHS powder was added to 100 ml of 2 wt% acetic acid solution while constant stirring and kept at room temperature for 24 h. To remove undissolved residual particles, the solution was filtered through a fritted glass disc filter, and the solution was left overnight to remove the air bubbles. On a clean glass plate the bubble-free, homogenous solution was spread by using a casting

knife in an atmosphere with no dust. After drying at room temperature for about 48 h, the membrane was peeled off and submerged in 50% alcoholic NaOH (0.1 M) solution for 24 h. Later washed with deionized water and annealed at 90 °C for 4 h. This membrane was labeled as PC-0. For the preparation of PECMs, the CHS membranes as prepared above were submerged in 3, 5, 7 and 9 mass % of PSSAMA solution at room temperature for 3 h and membranes were thoroughly washed with deaerated water and annealed for 3 h under vacuum oven at 90 °C. These PECMs were named as PC-1, PC-2, PC-3, and PC-4 and photographs of membrane are shown in Fig. 1. When tried to immerse CHS membranes in high mass % of PSSAMA solution, it resulted in a failed attempt because the membranes attained brittleness. The thickness of the membranes was found to be $40 \pm 2 \, \mu m$ by using a peacock dial thickness gauge (Model G, Ozaki Mfg. Co. Ltd., Japan). The reaction scheme for the development of PEC Membranes is shown in Scheme 1.

Characterizations

The structural interaction between CHS and PSSAMA were studied by Fourier transform infrared (FTIR) spectroscopy (Nicolet, impact 410, USA). The PECMs samples were consistently mixed with KBr and made as pellets under a hydraulic pressure of $400 \, kg/cm^2$ and scanned under a range of $400\text{-}4000 \, cm^{-1}$. The crystallographic phases of the PECMs were identified using wide-angle X-ray diffractometer (Brucker's D-8 advanced). The X-ray source was Ni-filtered CuK_{α} radiation (30 mA) and 40 kV of cathode current operation were applied. The PECMs samples were examined for 2θ values from the range of $5\text{-}50°$ at a constant speed of $8°/min$. Thermal performance of PECMs was assessed by thermogravimetry analysis (TGA) and differential scanning calorimetry (DSC) measurements (DSC Q 20, TA Instruments, Waters LLC, USA). 6–9 mg of PECMs samples were heated at the rate of $10 °C/min$ under nitrogen atmosphere. The morphology of PECMs was studied by scanning electron microscope (SEM) (JOEL Model JSM-6390 LV). Before taking SEM pictures, the membranes were dried at room temperature and then covered with thin layer of gold by a sputtering technique. Using a contact angle instrument (Kyowa Contact Angle Meter Model DMS-401, Japan), the change in the membrane hydrophilicity was evaluated. A drop of Milli-Q water was placed on the membrane surface and immediately after a drop of water was released on the surface, the droplet shape was recorded with a video camera. In order to determine the contact angle, Image analysis software (FAMS software) was used.

Ion-exchange capacity (IEC)

The IEC of the PECMs was measured using acid-base titration. PECMs samples were dried and recorded the weights. The dry PECMs samples were immersed in 10 ml of 1 N solution of Sodium chloride. After 24 h, this solution was used further to titrate against 0.01 N of Sodium hydroxide solutions. The IEC of the PECMs was
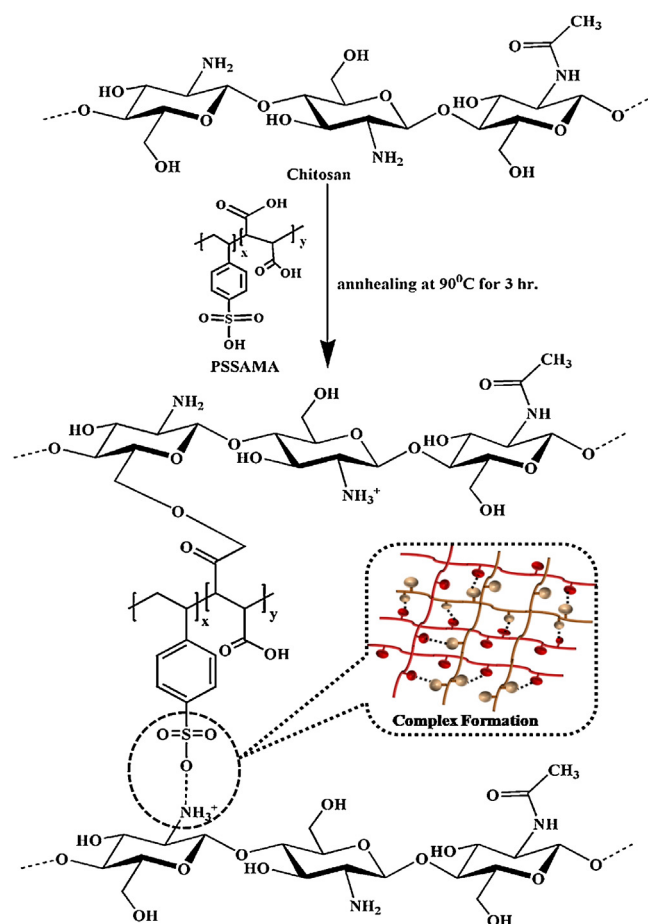
Scheme 1. Schematic presentation of ionic interactions between CHS and PSSMA.

been calculated as [7]:

$$IEC = \frac{A - E \times N_{NaOH} \times 2}{w} \tag{1}$$

where E is the amount of NaOH solution required to neutralize the equilibrated solution; A is the amount of NaOH solution required to neutralize the blank solution; 2 is the correction factor; the weight of membrane sample is denoted by w.

Determination of swelling degree

To study the swelling performance of the PECMs on time-dependent basis, samples were dried and weighed. The dried PECMs have been immersed in a known volume of azeotropic mixtures, i.e. water/isopropanol, water/1,4 dioxane, water/ter-butanol and water/n-propanol in an airtight glass jar at room temperature. After every 15 min, the swollen PECMs were weighed after careful blotting in a digital microbalance (Mettler, B204-S, Toledo — Switzerland). The constant swelling weights were

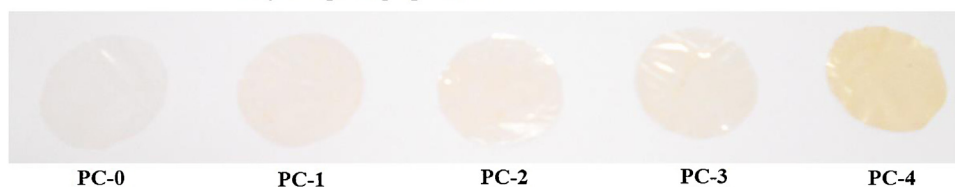**Physical photographs of PECMs**

Fig. 1. Physical photographs of PECMs.

obtained after 3 h; which ensures that the swollen PECMs reached an equilibrium state. The swelling degree percentage was calculated as [8]:

$$DS(\%) = \left(\frac{W_s - W_d}{W_d}\right) \times 100 \qquad (2)$$

where W_s is the swollen wet membrane mass (gram) and W_d is the dry membrane mass (gram) respectively.

Pervaporation experiments

The PV experiments have been carried out by the use of the equipment as shown in the Scheme 2(a) and (b) and (c). 34.23 cm^2 of operative surface area of the membrane was in contact with the feed mixture and the feed compartment capability was about 250 cm^3. The two stage vacuum pump (Toshniwal, Chennai, India) was used to keep the vacuum [1.333224×10^3 Pa (10 Torr)] on the downstream side of the equipment. In a feed compartment with a known volume of azeotropic compositions of water/isopropanol, water/1,4 dioxane, water/ter-butanol, and water/n-propanol the PECMs were enabled to equilibrate for 3 h, before performing the PV. Once PECMs attained a steady condition, permeate has been collected in a trap submerged in liquid nitrogen jar on the downstream facet. The experiments were conducted out at 30, 40, 50, and 60 °C. Thus, the obtained permeate was weighed on a digital microbalance to elucidate the flux. Compositions of water and organic solvents in permeate have been assessed by means of

figuring out the refractive index (RI) of permeate with a precision of ±0.0001 units using Abbe's refractometer (Atago-ST, Tokyo, Japan) and by means of comparing it with a standard graph of the refractive index, which was previously established with the known composition mixtures of water/isopropanol, water/1,4 dioxane, water/ter-butanol and water/n-propanol. All the experiments were conducted at least three times and the results were averaged. The results of azeotropic mixtures during course of PV were reproducible within the permissible range.

The capability of the membranes can be evaluated by means of total flux (J), separation factor (α_{sep}) and pervaporation separation index (PSI) [7].

$$J = \frac{W}{A.t} \qquad (3)$$

$$\alpha_{sep} = \frac{P_w/P_{org}}{F_w/F_{org}} \qquad (4)$$

$$PSI = J(\alpha_{sep} - 1) \qquad (5)$$

where W is permeate mass (kg); A is the area of effective membrane (m^2); t is the time for permeation (h); P_w and P_o are the mass percentage of water and organic solvents in the permeate respectively; F_w and F_o are the mass percentage of water and organic solvents in the feed mixture, respectively.
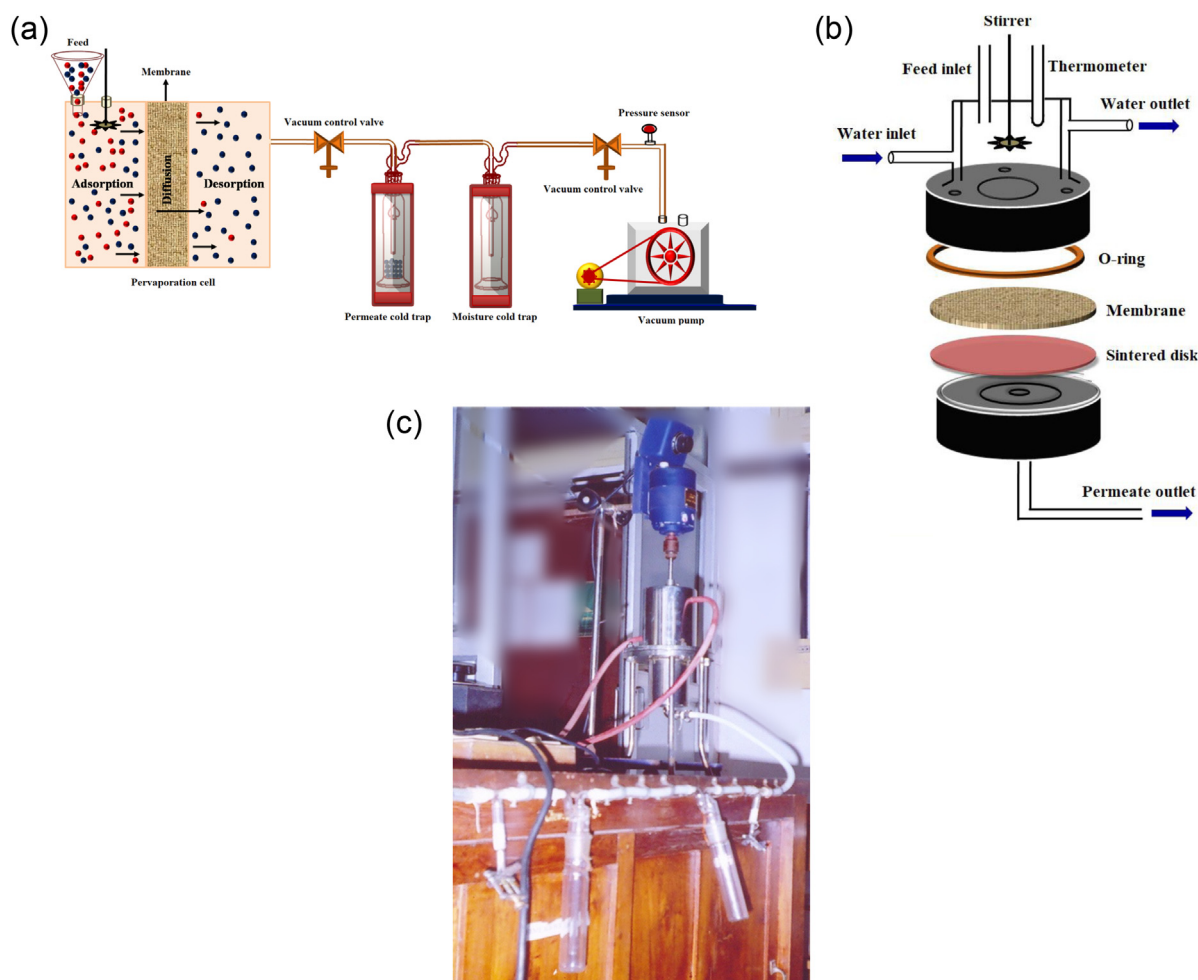
Scheme 2. (a) Schematic representation of pervaporation apparatus; (b) Schematic representation of PV cell; (c) Photograph of PV cell.

Results and discussion

Membrane characterization

FTIR

The FTIR spectra of CHS, PSSAMA, and PECMs are presented in Fig. 2. The CHS membrane shows the stretching vibrations at 3355 cm^{-1} and 1650 cm^{-1} attributed to —OH and —C=O stretching of the amide I band respectively [37,38]. Upon developing the PECMs by incorporating the PSSAMA via *ex-situ* method in the CHS matrix, the —OH band of CHS was moderately shifted to higher wave number at 3513 cm^{-1}. In addition, the intensity of this band was increased upon incorporation of the PSSAMA. This represents the formation of hydrogen bonding between —OH groups of CHS and —COOH groups of PSSAMA. In pure CHS membrane absorption band appears at 1558 cm^{-1} assigned for N—H (*N*-acetylated residues) amide II bending vibration of CHS [35,39,40]. The N—H bending vibration in PECM has shifted to a lower wave number showing a sharp peak at 1587 cm^{-1}. This clearly indicates the complex formation between the NH$_3^+$ group of CHS and —SO$_3$H group of PSSAMA. The absorption band at 1608 c^{-1} was observed in the pure PSSAMA assigned to —C=O group almost disappeared upon crosslinking and a new band appeared at 1723 cm^{-1} corresponds to an ester in the PECMs. A characteristic peak appeared at 1039 cm^{-1} in pure PSSAMA, which shows a presence of —SO$_3$ group in PSSAMA [36,7]. In pure CHS, C—H band is observed at 2927 cm^{-1}. The anti-symmetric stretching bands of C—O—C bridge and the skeletal vibration of C—O had been found at 1158 cm^{-1} and 1085 cm^{-1} respectively.

WAXD

WAXD is an effective tool for inspecting the degree of crystallinity and the structural modifications in polymer membranes. From the WAXD patterns (Fig. 3), it is noticed that CHS membrane (PC-0) showed two sharp diffraction peaks at $2\theta = 10°$ and 15°, and a broad peak at around 20° which are assigned to crystal form I, II and anhydrous form in the polymer [16]. It is observed that the intensity of CHS peaks were slowly reduced with the increase of PSSAMA mass percent. This is due to formation of ionic crosslinks between the amino groups of CHS and sulfonic groups of PSSAMA, which interrupt the hydrogen bonding forming between amino groups and hydroxyl groups of CHS and thus
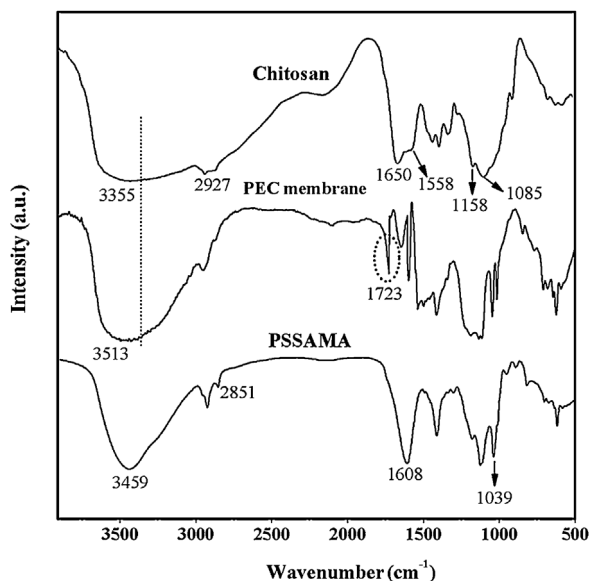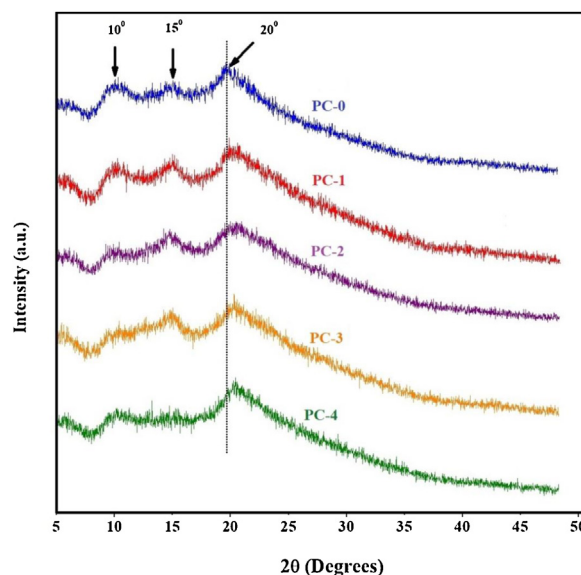

Fig. 3. WXRD patterns of CHS and PECMs: (PC-0) pure CHS; (PC-1) 3 mass% PSSAMA; (PC-2) 5 mass% PSSAMA; (PC-3) 7 mass% PSSAMA; (PC-4) 9 mass% PSSAMA.

decrease the extent of crystallinity in the PECMs. The position of the broad peak occurred at $2\theta = 20°$ was shifted slowly with increase of PSSAMA (PC-1 to PC-4). This could be evidenced by the calculated d-spacing values which are at the range of 4.372 to 4.250 Å. This is responsible for decreased intersegmental spacing due to shrinkage in cell size resulting, intermolecular interaction between —NH$_3^+$ group of CHS and —COOH/—SO$_3$H groups of PSSAMA, which make the membranes more rigid and compact that results in improved selective permeation [35].

TGA studies

The thermal stability of the CHS and PECMs was analyzed with TGA from room temperature to 650 °C at a heating rate of 10 °C/min under N$_2$ atmosphere. From Fig. 4 it could be seen that CHS membrane and PECMs undergo thermal decomposition in three stages at around 24–150 °C, 200–350 °C and above 350 °C. First weight loss up to 150 °C is intently related with the loss of adsorbed water molecules and acetic acid that correlates to around 20%

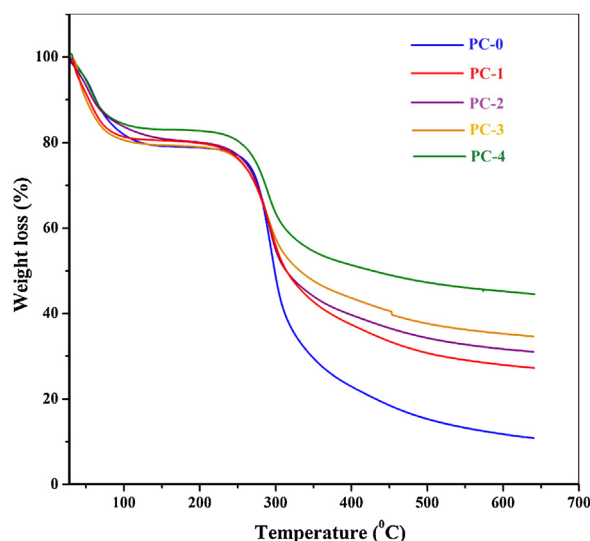**Fig. 2.** FTIR spectra of CHS, PSSAMA and PEC membrane.

Fig. 4. TGA of CHS and PECMs: PC-0, PC-1, PC-2, PC-3, PC-4.

weight loss [41]. Second weight loss of around 28–45% mass loss indicates major degradation peak of PECMs at 200–300 °C. This is due to degradation of sulfonic acid by desulfonation [7]. Third decomposition arises at 310–550 °C and above is presumably related to the degradation of the main chain backbones of PECMs. It is also found that the residual amounts of membranes were increased from PC-1 to PC-4 with an increase in PSSAMA content. In the present study the thermal stability of CHS membrane was increased with an increase in the mass % of PSSAMA content.

DSC studies

The thermal properties of the PECMs depends on the way of packing and structure of the polymer chain in the membrane, which is mainly represented by the T_g. Thermograms of CHS furnished in Fig. 5 showed a broad endothermic peak (T_g) at around 91 °C and the sharp exothermic peak (T_m) at 301 °C [42,43]. The thermograms of the PECMs showed a gradual shift in endothermic peaks from 91 °C to 101 °C by the increasing amount of PSSAMA in CHS matrix. This is generally due to the reducing the mobility of the polymer molecule which confirms the intermolecular interactions between PSSAMA and CHS membrane [44]. However, with increase in PSSAMA the melting temperature (T_m), in the membrane slightly changed which ranged from 302 °C to 307 °C for PC-1 to PC-4 membranes, respectively. This is because of the complex formation of PSSAMA and CHS in membrane matrix that forms a network which further improves the thermal stability and T_g in PECMs [45].

SEM studies

From SEM photographs (Fig. 6a), it can be spotted that surface views of CHS membrane and PECMs are even and homogenous with no appreciable clusters, no phase separation and no voids in the membrane matrix except a few clusters on PC-4. We can see the formation of few clusters on the membrane surface (PC-4) on surface views of SEM images of PECMs under high magnification (Fig. 7). This suggested that PECMs prepared in the present study are defects free and the homogeneity of the PECMs confirmed the ionic interaction existing between CHS and PSSAMA corresponding to complex formations. However, the membrane PC-4 with 9 mass % of PSSAMA showed few particles forming as clusters in the

membrane matrix. The cross-sectional views (Fig. 6b) displayed the neat CHS membrane with a smooth and compact surface as expected. Similarly, in PECMs, all the layers of the membrane are dense without any particles (PC-1 to PC-3), indicating a good compatibility between CHS and PSSAMA. The main reason for this is due a large number of sulfonic groups in PSSAMA, which definitely form strong ionic interactions and thus form strong interfacial bonds. Nevertheless, the rough surface can be seen in PC-4, which is likely due to poor dispersion and formation of agglomeration of PSSAMA at higher load. Obviously, this turns into responsible for the reduction in the permeation of molecules through the ionic crosslinked membranes.

Contact angle measurement

Hydrophilicity of the CHS and PECMs are studied by using contact angle measurement. Fig. 8 displays that CHS membrane shows contact angle of 80°. The lower values of contact angle indicated the hydrophilic nature of the membrane [46].

This hydrophilic nature of the pure CHS membrane is because of presence of —OH and —NH$_2$ groups in the CHS main chain. Inclusion of PSSAMA content in the pure CHS membrane decreases the hydrophilicity in PECMs, due to ionic crosslinking resulting in a decrease of —OH and —NH$_2$ groups thereby it outcomes in a higher contact angle measuring compare to the pure CHS membrane. These phenomena are in the same manner to the above mentioned FTIR and XRD results, as the increase in PSSAMA content in the membrane results in higher crosslinking density.

IEC studies

Fig. 9 displays the IEC of the CHS and PECMs. The IEC offers an evidence of ion-exchange groups available in the membranes. For pure CHS membrane, the IEC value is 0.13 meq/g. The IEC value of pure CHS is equal to the total number of free amine groups present in the membrane matrix. When the amount of PSSAMA in the membrane is increased, IEC values rise from 0.13 to 0.48 meq/g. This is due to the increasing ionic groups (—SO$_3$H and —COOH) in PECMs.

Swelling study

Sorption property of a membrane in the PV process performs a key role in accomplishing good separation performance [47,48], which is normally assessed by studying membrane swelling in different feed mixtures. Fig. 10 displays the swelling behavior of CHS membrane and PECMs in different azeotropic mixtures: water/ter-butanol, water/isopropanol, water/*n*-propanol and water/1,4 dioxane at 30 °C. With an increase in PSSAMA content in membranes PC-1 to PC-4 the degree of swelling has decreased. Reduction in swelling is mainly due to two effects: first is the effect of crosslinking: as membranes are crosslinked, the membranes would be more rigid and structurally compact and thus free volume available for water molecules would be decreased. The second is the effect of ionic interactions: the number of available water absorption sites (i.e, sulphonic acid) might be reduced as a result of strong complex formation between —SO$_3$H groups of PSSAMA and —NH$_2$ groups of CHS which leads to decreased chain mobility in the PECMs, hindering the access of water molecules [35]. From Fig. 10, we can see that the degree of swelling for different azeotropic mixtures are in the following manner: water/*n*-propanol > water/isopropanol > water/ter-butanol > water/1,4 dioxane. The affinity of azeotropic mixtures towards membranes is mainly based on polarity parameter (E_r) of the solvents in the azeotropic mixtures.

From Table 1, it is clear that *n*-propanol possess the highest polarity parameter and ability in formation of strong hydrogen bonding (proportional to the polarity parameter) [49] compared to
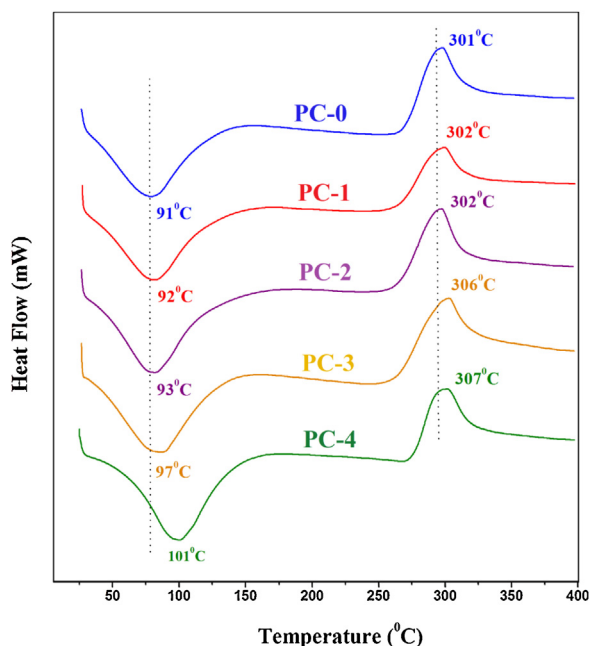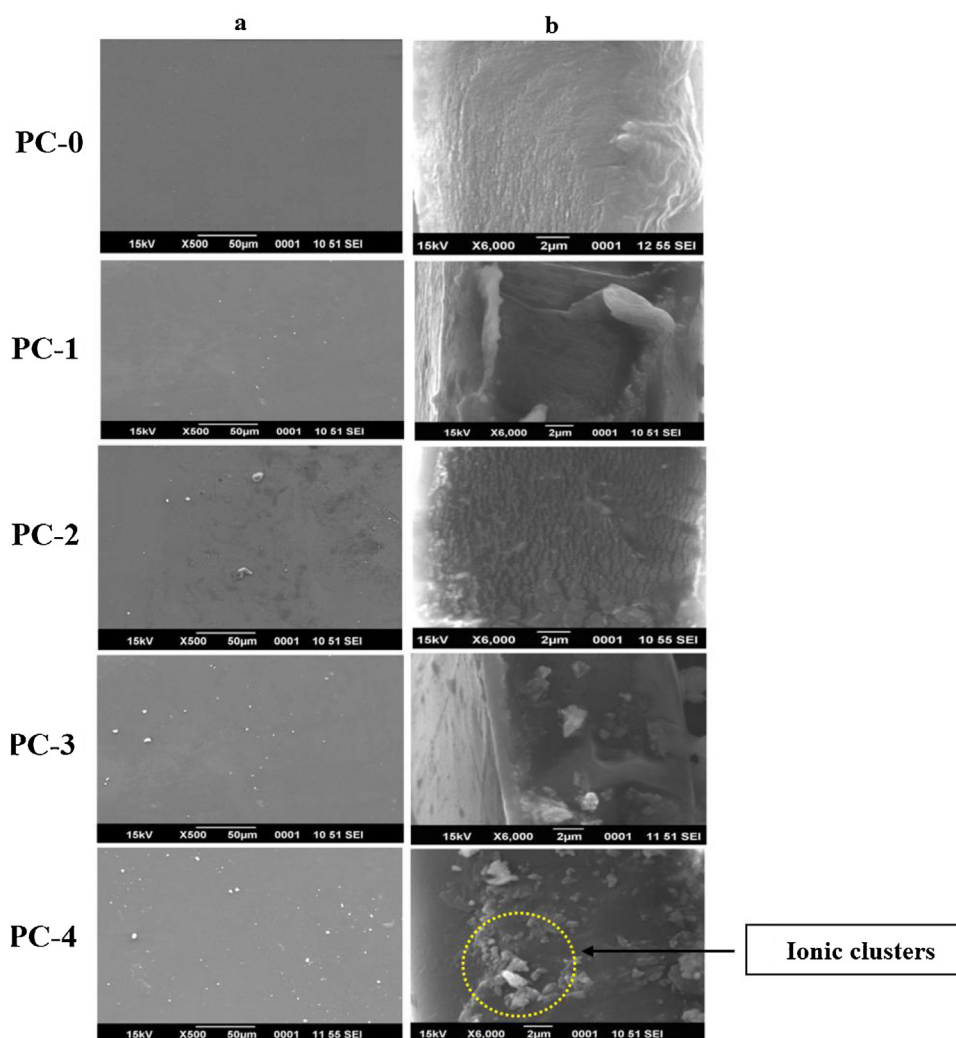
Fig. 5. DSC patterns of CHS and PECMs: PC-0, PC-1, PC-2, PC-3, PC-4.

Fig. 6. SEM micrographs pure CHS and PECMs of CHS: (PC-0) pure CS; (PC-1) 3 mass % PSSAMA; (PC-2) 5 mass % PSSAMA; (PC-3) 7 mass % PSSAMA; (PC-4) 9 mass % PSSAMA (a) surface view (b) cross-sectional view.

other three solvents, which implies that the interaction between membranes and *n*-propanol are through polar-polar groups and hydrogen bonds. In addition to this, the parameters such as density and dipole moment of n-propanol are high, compared to the other three solvents.

*Effect of different azeotropic mixtures and mass % of PSSAMA on PV*

Fig. 11 demonstrates the effect of different mass % of PSSAMA on the total permeation flux of prepared PECMs at 30 °C in dehydrating water/ter-butanol, water/*n*-propanol, water/isopropanol and water/1,4 dioxane mixtures at their azeotropic point. It can be noted that the permeation flux was decreased from PC-0 to PC-4 owing to the increased crosslinking and complex formation with an increase of PSSAMA content, as discussed in the swelling study. Decline in flux, can also be supported by contact angle measurements.

From Fig. 11 we can see that water/ter-butanol mixture shows the highest flux, followed by water/*n*-propanol, water/isopropanol, and water/1,4 dioxane. The trend of permeation flux for azeotropic mixtures is instinctively contrary to the trend of swelling study. The first reason is that the azeotropic mixture of water/ter-butanol (11.76 wt% of water and 88.24 wt% of ter-butanol) having greater hydrocarbon content of the alcohol weakens the hydrogen bonding between the alcohol and the water molecules. Thus, water

molecules are easily separated from water/ter-butanol mixtures by the membrane when pressure (vacuum) is applied downstream side of the membrane. Second reason is that ter-butanol has a more bulky structure that is more resistant when diffused through the membrane, while the water molecule can be diffused through the membrane and easily separated out [50].

The permeation flux for water/*n*-propanol and water/isopropanol mixtures is less than water/ter-butanol mixture. This is because of the interaction between alcohol and water. Both *n*-propanol and isopropanol are polar in nature; they are forming the strong hydrogen bonding between water molecules. This prevents the diffusion of water molecules through membrane and produces less flux than water/ter-butanol mixture. Water/1,4 dioxane mixture shows less flux than the above three water/alcohol mixtures. Because 1, 4 dioxane is a heterocyclic and less polar in nature. The presence of the aromatic ring in 1,4 dioxane increases the hydrophobicity of the mixture, which causes a reduction in the diffusion of water molecules through membrane.

Fig. 12 shows the impact of different mass % of PSSAMA content on selectivity for water/ter-butanol, water/*n*-propanol, water/isopropanol and water/1,4 dioxane mixtures for all PECMs. From membranes PC-0 to PC-4 the separation factor linearly improved by increasing the mass % of PSSAMA content. Firstly, it is ascribed due to the formation of crosslinking between the —OH group of CHS and the —COOH group of PSSAMA. Secondly, with an increase
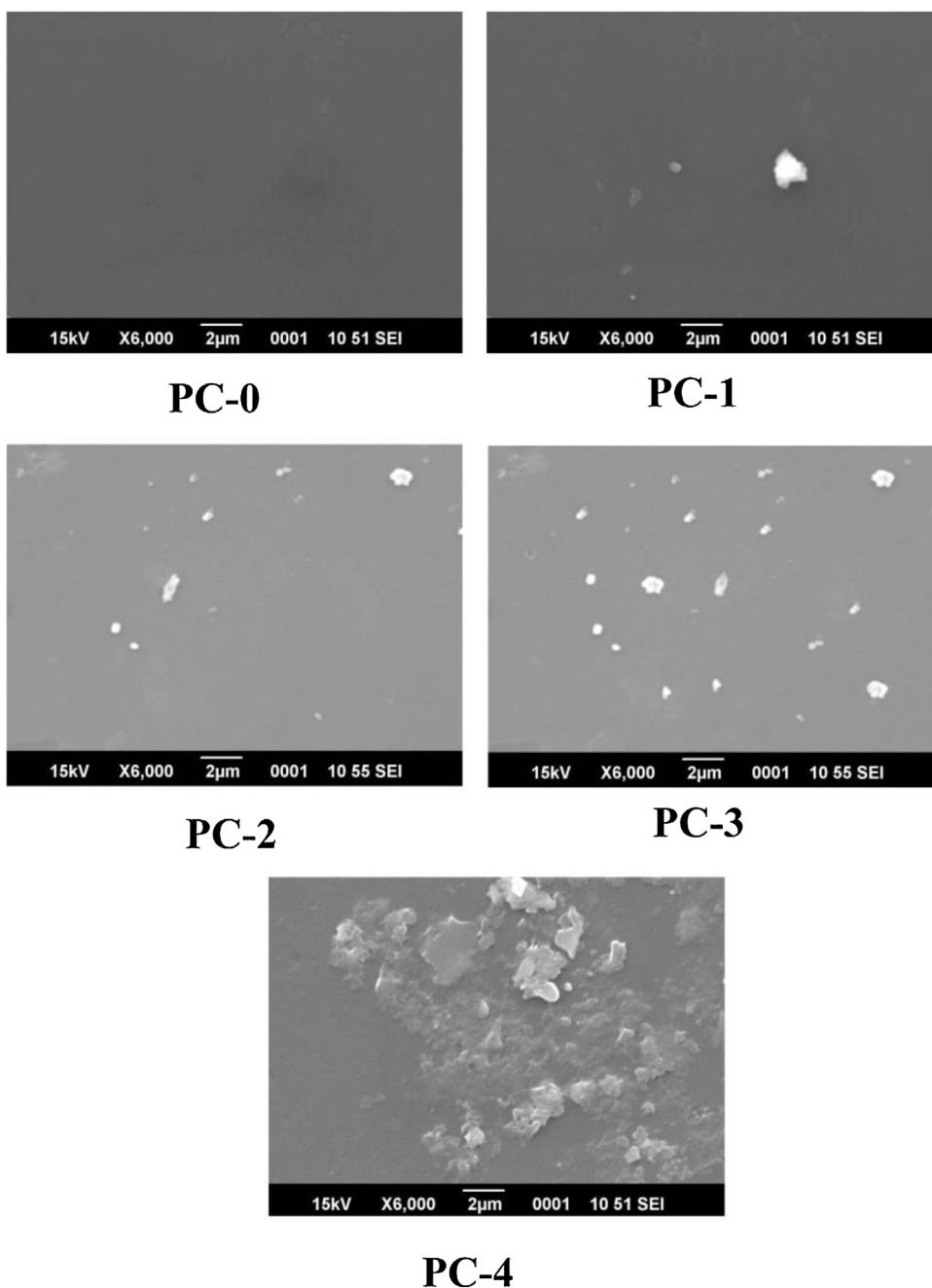
Fig. 7. High magnification surface views of SEM micrographs pure CHS and PECMs of CHS: (PC-0) pure CS; (PC-1) 3 mass % PSSAMA; (PC-2) 5 mass % PSSAMA; (PC-3) 7 mass % PSSAMA; (PC-4) 9 mass % PSSAMA.

in PSSAMA, there is increase in hydrogen bond formation and electrostatic force of attraction due to which compactness and rigidity of the membrane increases. This is also supported by d-spacing values mentioned in WAXD section. When comparing membranes performances in terms of selectivity for water/ter-butanol, water/*n*-propanol, water/isopropanol, and water/1,4 dioxane mixtures the largest selectivity values are observed for water/ter-butanol mixture due to the low affinity of ter-butanol molecules towards PECMs and the presence of steric effect caused by bulky groups present in the ter-butanol that leads to effective separation of water from water/ter-butanol mixture.

The water/isopropanol and water/*n*-propanol azeotropic mixtures showed the low selectivity than the water/ter-butanol
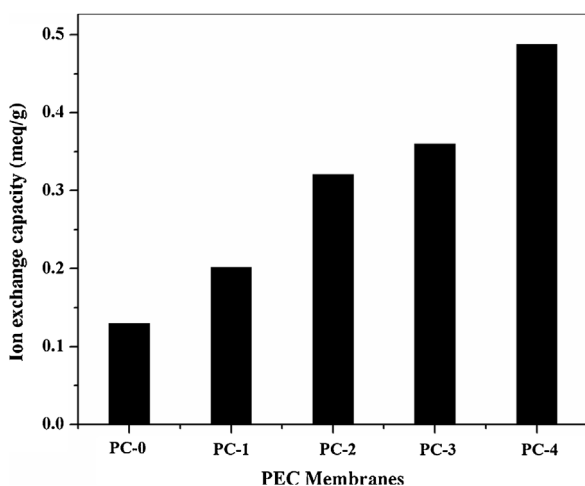
mixture for all the PECMs. A lower selectivity is due to the membrane's high degree of swelling in mixtures. However, increased swelling was a negative effect on membranes selectivity subsequently swollen and plasticized upstream membrane layer permits some *n*-propanol and isopropanol molecules also to escape into permeate along with water [51]. The water/1,4 dioxane mixture shows the lowest selectivity among the three azeotropic mixtures. This is because of the aliphatic segment of 1, 4 dioxane and it's small dipole moment which results in penetration of 1,4 dioxane molecule into the semicrystalline domain of the membrane and diffusion through the pores of the membrane.

The extent of permeation of individual components was evaluated with the aid of plotting the total flux, fluxes of water
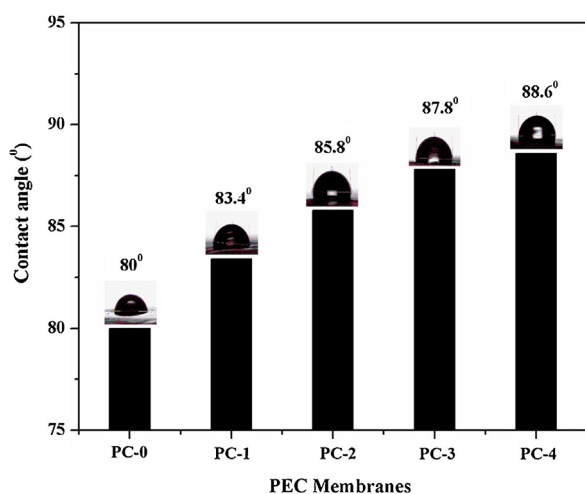
Fig. 8. Graphical representation of Contact angle measurements for pure CHS and PECMs of CHS: (PC-0) pure CS; (PC-1) 3 mass % PSSAMA; (PC-2) 5 mass % PSSAMA; (PC-3) 7 mass % PSSAMA; (PC-4) 9 mass % PSSAMA.

Fig. 10. The swelling behavior of membranes (PC-0 to PC-4) in water/ter-butanol, water/isopropanol, water/n-propanol and water/1,4 dioxane mixtures of their azeotropic composition.
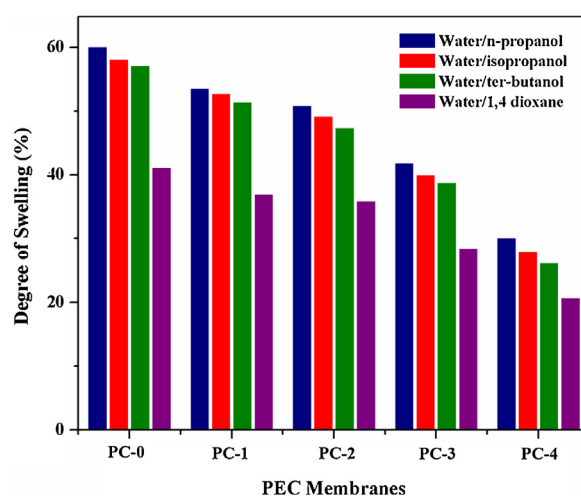

Fig. 9. Ion Exchange Capacity for pure CHS and PECMs of CHS: (PC-0) pure CS; (PC-1) 3 mass % PSSAMA; (PC-2) 5 mass % PSSAMA; (PC-3) 7 mass % PSSAMA; (PC-4) 9 mass % PSSAMA.

and ter-butanol as a function of mass % of PSSAMA content in the membrane for the azeotropic composition of the mixture as shown in Fig.13. Total flux and the flux of water overlap each other for all PSSAMA incorporated membranes, indicating that all PECMs are selective towards water. Membrane separation ability can be determined by pervaporation separation index (PSI) of the membranes. It has been used to evaluate the overall membrane pervaporation performance. The calculated values at the azeotropic point for water/ter-butanol at 30 °C are included in Fig. 13. It reveals that the PSI value of the PECMs (PC-0 to PC-4) has been increased by increasing the amount of PSSAMA. This was due to the formation of PECs between CHS and PSSAMA, which was discussed in both swelling and permeation studies.

Diffusion coefficients

In the separation process, the diffusion step controls the transport of penetrants by establishing a fast equilibrium distribution between the bulk feed and the upstream surface of a membrane [52]. Therefore, it is obviously important to estimate the diffusion coefficient of penetrating molecules in order to understand the mechanism of molecular transport. From Fick's diffusion law [53]:

$$J_i = -D_i \frac{dC_i}{dx} \quad (6)$$

J — permeation flux per unit area (kg/m² s), D — diffusion coefficient (m²/s), C — permeant concentration (kg/m³), subscript i stands for water or IPA, and x — diffusion length (m). Thus, equation for D_i [47]:

$$D_i = \frac{J_i \delta}{C_i} \quad (7)$$

where δ is the thickness of membrane. Table 2 presents the calculated values of D_i for four different azeotropic systems at their azeotropic point at 30 °C.
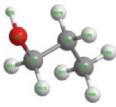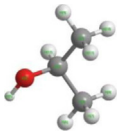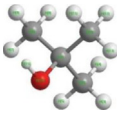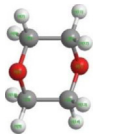
Similar to the PV study, the diffusion coefficients of water and organics decreased considerably from membrane PC-1 to PC-4 due to increase of compactness in the membrane matrix. The comparison of the diffusion coefficient of four different azeotropic mixtures (Table 2) shows that the water/ter-butanol mixture shows the highest diffusion coefficient. This is because water/ter-butanol has a greater hydrocarbon content of the alcohol at their azeotropic point and it weakens the hydrogen bonding between the alcohol and the water molecules. Due to this, water molecules are easily diffused through the membrane and separated out. Despite this, the magnitude of the diffusion coefficients of water is quite high in comparision to that of other organics, indicating that the PECMs are still selective towards water molecules.

Temperature effect on PV performance

The PV performance for four different azeotropic mixtures has been studied for all the PECMs at 30 °C, 40 °C, 50 °C and 60 °C at their azeotropic point has given the values in Tables 3–6.

Table 3, shows that the permeation rate has been increased with increase in temperature with decrease in the separation selectivity. Once the temperature increases, the intermolecular and intramolecular interactions occurring between permeants and membrane materials decreases resulting in plasticization effect. Due to plasticization effect along with water molecules ter-butanol molecules also diffuse through the membrane which in turn decreases the selectivity.

Table 1
Physical properties of *n*-propanol, isopropanol, ter-butanol, and 1,4 dioxane.

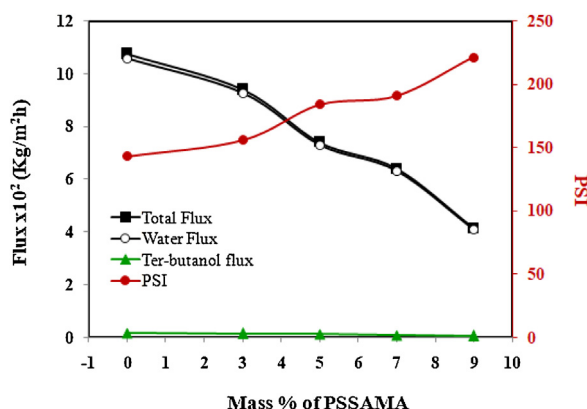| Properties	*n*-Propanol	Isopropanol	Ter-butanol	1,4 Dioxane
Molecular formula	C_3H_8O	C_3H_8O	$C_4H_{10}O$	$C_4H_8O_2$
Structure				
Molar mass (g/mol)	60.09	60.10	74.12	88.11
Density (g/cm^3)	0.803	0.786	0.781	1.03
Boiling point (°C)	97	82.6	82.2	101
Polarity parameter E_r (30)[21](kcal/mol)	50.7	48.4	43.3	36.0
Dipole moment (D)	3.09	1.66	1.66	0.45
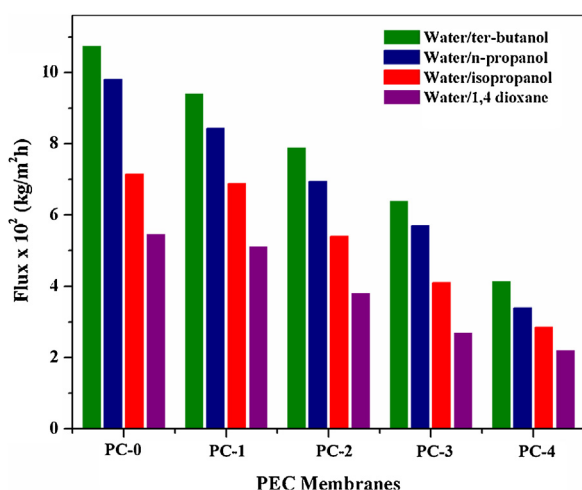
Fig. 11. Effect of different mass% of PSSAMA on total permeation flux in water/ter-butanol, water/isopropanol, water/*n*-propanol and water/1,4 dioxane mixtures at their azeotropic composition.
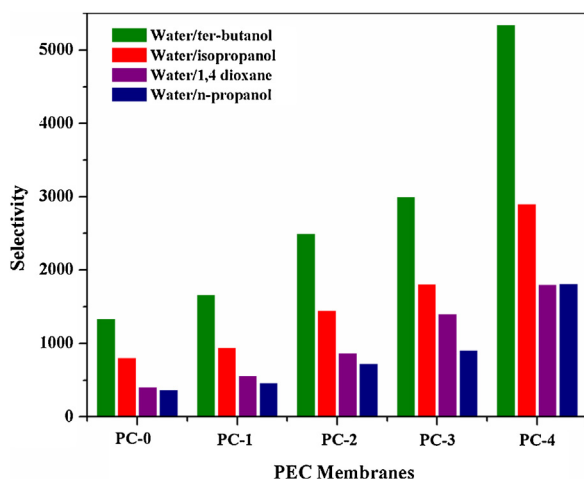
Fig. 13. Effect of different mass % of PSSAMA on total flux, water and ter-butanol flux and PSI for water/ter-butanol mixture.

And also from Tables 4–6 we can see as the temperature increases along with water molecules *n*-propanol, isopropanol and 1,4 dioxane molecules also permeates as a result selectivity decreases. The only reason is with increase in temperature the flexibility and softness in polymer matrix increases.

In order to estimate the activation energies for permeation and diffusion we have used the Arrhenius type equation [42]:

$$X = X_0 \exp\left(\frac{-E_x}{RT}\right) \tag{8}$$

X- Permeation (*J*) or Diffusion (*D*), X_o — a constant representing a pre-exponential factor of J_o or D_o, E_x — activation energy for permeation or diffusion depending upon the transport process, R — gas constant, T — temperature (K). Figs. 14 and 15 show Arrhenius log *J* and log D versus temperature for all PECMs in the water/ter-butanol azeotropic mixture, respectively.

The straight lines in all the cases, signifying that permeability and diffusivity follows the Arrhenius equation. The activation energies for total permeation (E_p) and diffusion (E_d) were calculated from the linear plots of least-square fits. Similarly, activation energies for water permeation (E_{pw}), ter-butanol (E_{pTBOH}), *n*-propanol (E_{pNPA}), isopropanol (E_{pIPA}), 1,4 dioxane (E_{pDIO}) and diffusion of water (E_{Dw}) have been calculated, but the plots are not given to avoid the over crowdedness. Table 7 shows the calculated values for the water/ter-butanol azeotropic mixture.

A large difference was noticed between the activation energy values of water (E_{pw}) and ter-butanol (E_{pTBOH}), indicating that membranes have higher water separation efficiency. The

Fig. 12. Effect of different mass% of PSSAMA on selectivity in water/ter-butanol, water/isopropanol, water/*n*-propanol and water/1,4 dioxane mixtures of their azeotropic composition.

Table 2
Diffusion coefficients of water/ter-butanol, water/n-propanol, water/isopropanol, water/1,4 dioxane azeotropic mixture at their azeotropic point at 30 °C.

Azeotropic system	$D_w \times 10^8$ (cm²/s)					$D_{org} \times 10^9$ (cm²/s)				
	PC-0	PC-1	PC-2	PC-3	PC-4	PC-0	PC-1	PC-2	PC-3	PC-4
water/ter-butanol	18.6	16.4	12.8	11.1	7.13	0.56	0.39	0.2	0.14	0.05
water/isopropanol	11.9	11.5	8.07	6.84	4.75	0.48	0.4	0.18	0.12	0.05
water/n-propanol	6.96	5.99	4.96	4.15	2.33	0.63	0.43	0.22	0.15	0.04
water/1,4 dioxane	6.02	5.65	3.75	2.99	2.44	0.78	0.49	0.21	0.1	0.06

Table 3
Pervaporation flux and separation selectivity of PECMs for water/ter-butanol mixture at different temperatures.

Temp. (ºC)	$J \times 10^2$ (kg/m² h)					$\alpha_{\sigma\varepsilon\pi}$				
	PC-0	PC-1	PC-2	PC-3	PC-4	PC-0	PC-1	PC-2	PC-3	PC-4
30	10.75	9.41	7.4	6.39	4.14	1332	1659	2493	2993	5352
40	11.95	10.8	7.88	7.15	4.82	930	1435	2136	2337	3403
50	12.26	11.1	9.2	7.85	5.81	742	1202	1493	1868	2993
60	12.3	11.72	9.44	8.76	6.42	728	930	1243	1493	2337

Table 4
Pervaporation flux and separation selectivity of PECMs for water/n-propanol mixture at different temperatures.

Temp. (ºC)	$J \times 10^2$ (kg/m² h)					α_{sep}				
	PC-0	PC-1	PC-2	PC-3	PC-4	PC-0	PC-1	PC-2	PC-3	PC-4
30	9.80	8.44	6.97	5.84	3.28	359	457	720	901	1806
40	10.66	8.91	7.45	6.73	4.54	322	419	630	788	1263
50	11.07	9.60	8.37	7.16	4.97	285	387	560	663	1148
60	11.10	9.64	8.49	7.76	5.06	282	359	503	600	1052

Table 5
Pervaporation flux and separation selectivity of PECMs for water/isopropanol mixture at different temperatures.

Temp. (ºC)	$J \times 10^2$ (kg/m² h)					α_{sep}				
	PC-0	PC-1	PC-2	PC-3	PC-4	PC-0	PC-1	PC-2	PC-3	PC-4
30	7.10	6.88	4.83	4.10	2.85	799	936	1445	1800	2898
40	8.44	7.50	5.53	5.42	3.86	711	799	1164	1313	2262
50	8.79	8.34	6.23	6.00	4.93	653	719	1030	1203	1722
60	9.12	9.02	7.27	6.59	5.40	624	704	900	1030	1313

Table 6
Pervaporation flux and separation selectivity of PECMs for water/1,4 dioxane mixture at different temperatures.

Temp. (ºC)	$J \times 10^2$ (kg/m² h)					α_{sep}				
	PC-0	PC-1	PC-2	PC-3	PC-4	PC-0	PC-1	PC-2	PC-3	PC-4
30	5.46	5.11	3.39	2.70	2.20	400	557	860	1401	1794
40	5.74	5.62	3.96	3.37	2.44	355	495	721	657	1245
50	5.98	5.87	4.64	3.57	2.70	341	436	620	620	932
60	6.12	5.99	4.74	4.37	4.25	321	400	557	495	557

activation energy values for permeation of water (E_{pw}) and total permeation(E_p) are close to each other, indicating that the combined transport of both water and ter-butanol molecules is minimal because of higher selective nature of membranes. The activation energy values have been increased from membrane PC-0 to PC-4, due to increased rigidity and compactness in the membrane due to the increased crosslinking density, the hydrogen bonding and PEC formation. The assessed E_p values ranged from 12.63 to 3.65 kJ/mol, and E_D values ranged from 12.82 to 3.77 kJ/mol. By these values, we have further calculated the heat of sorption as [47]:
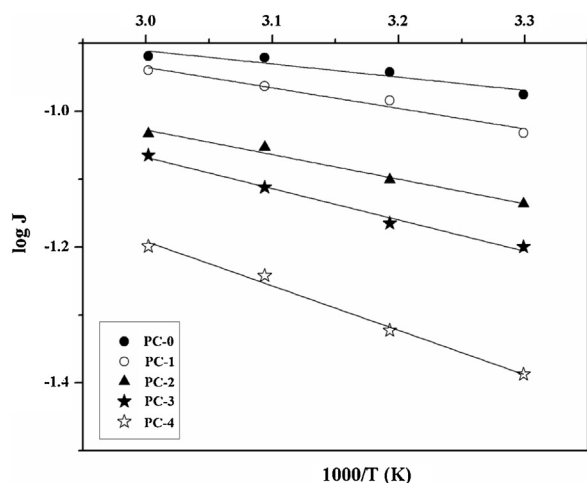
$$\Delta H_s = E_p - E_D \tag{9}$$

Fig. 14. Effect of PSSAMA content in PEC membranes on log J with in water/ter-butanol azeotropic mixture.
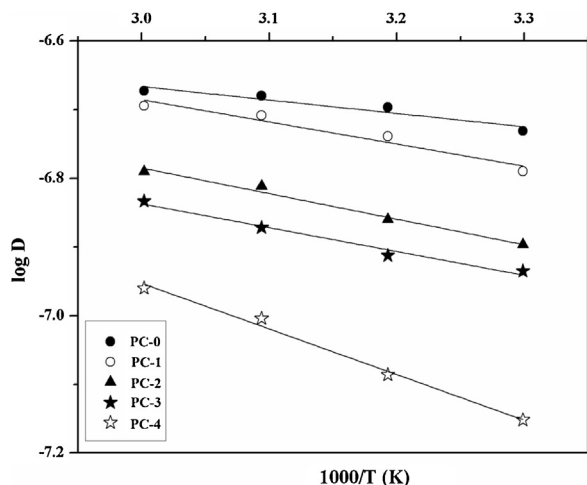

Fig. 15. Effect of PSSAMA content in PEC membranes on log D with in water/ter-butanol azeotropic mixture.

Table 7
Arrhenius activation parameter for permeation, diffusion, and heat of sorption in water/ter-butanol mixture.

Parameters (kJ/mol)	PC-0	PC-1	PC-2	PC-3	PC-4
E_P	3.65	5.8	7.44	8.71	12.63
E_D	3.77	5.98	7.62	8.9	12.82
E_{pw}	3.52	5.7	7.35	8.64	12.58
E_{pTBOH}	20.8	21.71	27.87	28.05	34.63
E_{Dw}	3.64	5.89	7.54	8.84	12.78
ΔH_σ	−0.12	−0.18	−0.18	−0.19	−0.19

The transportation of molecules through the polymer matrix provides additional information on ΔH_s values [29]. In the present study, the ΔH_s values (Table 7) obtained for all the membranes are negative, signifying that Langmuir's sorption is predominant, giving an exothermic contribution.

Conclusions

PECMs were prepared by *ex-situ* crosslinking of CHS with different mass % of PSSAMA for the separation of azeotropic water/ter-butanol, water/*n*-propanol, water/isopropanol and water/1,4 dioxane mixtures. The polyelectrolyte complex formation in the CHS polymer is confirmed by FTIR. Thermal stability of PECMs was higher than CHS membrane. A reduction of permeation flux and an increase in separation selectivity was observed with increase of the PSSAMA mass proportion in the membrane matrix. This was clarified based on decreased membrane swelling and free-volume because of formation of complex between CHS and PSSAMA. When we compared the membrane performance in terms of flux for water/ter-butanol, water/*n*-propanol, water/isopropanol and water/1,4 dioxane mixtures; water/ter-butanol showed the highest flux. Since the azeotropic point of water/ter-butanol having greater hydrocarbon content of alcohol, weakens the hydrogen bond between the alcohol and the water molecules. Correlation of selectivity for water/ter-butanol, water/*n*-propanol, water/isopropanol and water/1,4 dioxane mixtures, the most elevated selectivity esteems are observed for water/ter-butanol due to the low affinity of ter-butanol molecules towards PECMs and the presence of steric effect caused by bulky groups present in the ter-butanol. For the azeotropic water/ter-butanol mixture the membrane containing 9 mass % of PSSAMA showed the separation selectivity of 5352 with a flux of 4.145×10^{-2} kg/m^2 h at 30 °C. The PECMs were used to separate the azeotropic mixtures at 30, 40, 50, and 60 °C. The total permeation flux increased with the increase in the feed temperature, while the selectivity decreased. The PECMs shows significantly more than two-fold lower activation energy values for water permeation (E_{pw}) than that of organics (E_{po}), suggesting that the membranes prepared in the present work have higher separation capability for water. The PECMs showed negative heat of sorption values, indicating that sorption is predominated by the Langmuir's mode of sorption, which gives an exothermic contribution. The developed PECMs in this work are accordingly excellent candidates for the dehydration of azeotropic mixtures.

Conflict of interest

None of the author has proclaimed any conflict of interest.

Acknowledgments

References

[1] M. Zhu, J. Qian, Q. Zhao, Q. An, Y. Song, Q. Zheng, J. Membr. Sci. 378 (2011) 233.
[2] G. Dudek, M. Gnus, R. Turczyn, A. Strzelewicz, M. Krasowska, Sep. Purif. Technol. 133 (2014) 8.
[3] W. Yang, T. Muhammad, A. Yigaimu, K. Muhammad, L. Chen, J. Sep. Sci. 41 (2019) 4185.
[4] X.S. Wang, Q.F. An, Q. Zhao, K.R. Lee, J.W. Qian, C.J. Gao, J. Membr. Sci. 435 (2013) 71.
[5] G. Wu, J. Ma, S. Li, J. Guan, B. Jiang, L. Wang, J. Li, X. Wang, L. Chen, J. Colloid Interface Sci. 528 (2018) 360.
[6] T. Liu, Q.F. An, Q. Zhao, K.R. Lee, B.K. Zhu, J.W. Qian, C.J. Gao, J. Membr. Sci. 429 (2013) 181.
[7] P.S. Rachipudi, A.A. Kittur, A.M. Sajjan, R.R. Kamble, M.Y. Kariduraganavar, Chem. Eng. Sci. 94 (2013) 84.
[8] A.M. Sajjan, M.Y. Kariduraganavar, J. Membr. Sci. 438 (2013) 8.
[9] I. Cabasso, Ind. Eng. Chem. Prod. Res. Dev. 22 (1983) 313.
[10] Y. Wang, L. Jiang, T. Matsuura, T.S. Chung, S.H. Goh, J. Membr. Sci. 318 (2008) 217.
[11] L. Wang, J. Li, Y. Lin, C. Chen, J. Membr. Sci. 305 (2007) 238.
[12] P.S. Rachipudi, A.A. Kittur, A.M. Sajjan, M.Y. Kariduraganavar, J. Membr. Sci. 441 (2013) 83.
[13] A.R. Bagheri, M. Arabi, M. Ghaedi, A. Ostovan, X. Wang, J. Li, L. Chen, Talanta 195 (2019) 390.
[14] H. Liu, Y. Wang, Yue Yu, W. Chen, L. Jiang, J. Qin, J. Biomed. Mater. Res. Part B. 9999B (2019) 1.

[15] H. Peng, H. Xiong, J. Li, M. Xie, Y. Liu, C. Bai, L. Chen, Food Chem. 121 (2010) 23.
[16] J.G. Varghese, A.A. Kittur, P.S. Rachipudi, M.Y. Kariduraganavar, J. Membr. Sci. 364 (2010) 111.
[17] Q. Zhao, Q.F. An, Y. Ji, J. Qian, C. Gao, J. Membr. Sci. 379 (2011) 19.
[18] X.S. Wang, Q.F. An, T. Liu, Q. Zhao, W.S. Hung, K.R. Lee, C.J. Gao, J. Membr. Sci. 452 (2014) 73.
[19] J.J. Shieh, R.Y.M. Huang, J. Membr. Sci. 127 (1997) 185.
[20] S.G. Kim, K.S. Lee, K.H. Lee, J. Appl. Polym. Sci. 103 (2007) 2634.
[21] S.G. Kim, H.R. Ahn, K.H. Lee, Curr. Appl. Phys. 9 (2009) e42.
[22] J. Lukas, K. Richau, H.H. Schwarz, D. Paul, J. Membr. Sci 106 (1995) 281.
[23] H.H. Schwarz, J. Lukas, K. Richau, J. Membr. Sci. 218 (2003) 1.
[24] Y.F. Li, H.P. Jia, Q.L. Cheng, F.S. Pan, Z.Y. Jiang, J. Membr. Sci. 375 (2011) 304.
[25] J. Meier-Haack, W. Lenk, D. Lehmann, K. Lunkwitz, J. Membr. Sci. 184 (2001) 233.
[26] W. Lenk, J. Meier-Haack, Desalination 148 (2002) 11.
[27] G.J. Zhang, N.X. Wang, X. Song, S.L. Ji, Z.Z. Liu, J. Membr. Sci. 338 (2009) 43.
[28] G.J. Zhang, X. Gao, S.L. Ji, Z.Z. Liu, Mater. Sci. Eng. C 29 (2009) 1877.
[29] Q. Zhao, J.W. Qian, Q.F. An, Q. Yang, P. Zhang, J. Membr. Sci. 320 (2008) 8.
[30] Q. Zhao, J.W. Qian, Q.F. An, Q. Yang, Z.L. Gui, ACS Appl. Mater. Interfaces 1 (2009) 90.
[31] Q. Zhao, J.W. Qian, Q.F. An, Z.L. Gui, H.T. Jin, M.J. Yin, J. Membr. Sci. 329 (2009) 175.
[32] Q. Zhao, J.W. Qian, Q.F. An, C. Gao, Z. Gui, H. Jin, J. Membr. Sci. 333 (2009) 68.
[33] P.S. Rachipudi, A.A. Kittur, S.K. Choudhari, J.G. Varghese, M.Y. Kariduraganavar, Eur. Polym. J. 45 (2009) 3116.
[34] S.K. Choudhari, H.G. Premakshi, M.Y. Kariduraganavar, Polym. Eng. Sci. 56 (2016) 715.
[35] J.A. Seo, J.H. Koh, D.K. Roh, J.H. Kim, Solid State Ionics 180 (2009) 998.
[36] D.S. Kim, M.D. Guiver, S.Y. Nam, T.I. Yun, M.Y. Seo, S.J. Kim, H.S. Hwang, J.W. Rhim, J. Membr. Sci. 281 (2006) 156.
[37] H. Peng, H. Xiong, J. Li, L. Chen, Q. Zhao, J. Food Eng. 101 (2010) 113.
[38] A. Ostovan, M. Ghaedi, M. Arabi, Q. Yang, J. Li, Lingxin Chen, ACS Appl. Mater. Interfaces 10 (2018) 4140.
[39] L. Wang, J. Li, J. Wang, X. Guo, X. Wang, J. Choo, L. Chen, J. Colloid Interface Sci. 541 (2019) 376.
[40] W. Lu, J. Li, Y. Sheng, X. Zhang, J. You, L. Chen, J. Colloid Interface Sci. 505 (2017) 1134.
[41] M.Z. Borowska, D. Chełminiak, H. Kaczmarek, A.K. Kedziera, J. Therm. Anal. Calorim. 124 (2016) 1267.
[42] A.M. Sajjan, H.G. Premakshi, M.Y. Kariduraganavar, J. Ind. Eng. Chem. 25 (2015) 151.
[43] F.S. Pereira, D.L.S. Agostini, A.E. Job, E.R.P. González, J. Therm. Anal. Calorim. 114 (2013) 321.
[44] R.K. Mishra, S. Mondal, M. Datt, A.K. Banthia, Int. J. Plast. Technol. 14 (2010) 80.
[45] H.G. Premakshi, K. Ramesh, M.Y. Kariduraganavar, Chem. Eng. Res. Des. 94 (2015) 32.
[46] S.S. Shenvi, S.A. Rashid, A.F. Ismail, M.A. Kassim, A.M. Isloor, Desalination 315 (2013) 135.
[47] P.S. Rachipudi, M.Y. Kariduraganavar, A.A. Kittur, A.M. Sajjan, J. Membr. Sci. 383 (2011) 224.
[48] P.J. Flory, J. Rehner, J. Chem. Phys. 11 (1943) 521.
[49] X. Qiao, T.S. Chung, J. Ind. Eng. Chem. 44 (2005) 8938.
[50] W.F. Guo, T.S. Chung, T. Matsuura, J. Membr. Sci. 245 (2004) 199.
[51] S.S. Binduru, S. Sridhar, G.S. Murthy, S. Mayor, J. Chem. Technol. Biotechnol. 80 (2005) 1416.
[52] A.A. Kittur, M.Y. Kariduraganavar, U.S. Toti, K. Ramesh, T.M. Aminabhavi, J. Appl. Polym. Sci. 90 (2003) 2441.
[53] A. Yamasaki, T. Iwatsubo, T. Masuoka, K. Mizoguchi, J. Membr. Sci. 89 (1994) 111.